Research Article | Vol. 4, No. 5 / 15 May 2021 / OSA Continuum 1488

Ultraslow Kuznetsov-Ma solitons and Ahkmediev breathers in a cold three-state medium exposed to nanosecond optical pulses

WANWAN WANG,[1] LILI BU,[1] DANDAN CHENG,[1] YANLIN YE,[1] SHIHUA CHEN,[1,3] AND FABIO BARONIO[2,4]

[1]School of Physics and Quantum Information Research Center, Southeast University, Nanjing 211189, China
[2]INO CNR and Dipartimento di Ingegneria dell'Informazione, Università di Brescia, Via Branze 38, 25123 Brescia, Italy
[3]cshua@seu.edu.cn
[4]fabio.baronio@unibs.it

Abstract: We investigate the formation of the Kuznetsov-Ma solitons and Ahkmediev breathers in a cold Λ-type three-level atomic system that interacts with a probe field of nanosecond pulse duration and a strong continuous-wave driving field via an electromagnetically induced transparency process. Within the framework of the Hirota equation, exact explicit analytical solutions of these breathers are obtained, showing different amplitude and oscillatory characteristics. Numerical simulations confirm the stability of both types of breathers against non-integrable perturbations that are caused by the nonvanishing decay rates of atomic states. We show that both breathers thus generated can propagate at a quite low group velocity.

1. Introduction

The breathers on a finite background have attracted increasing attention in many fields including hydrodynamics and optics [1,2], due to their intimate connection to the formation of extreme rogue wave events [3,4]. One type of such breathers is the Kuznetsov-Ma (KM) soliton [5,6], which behaves like an ordinary soliton, localized yet oscillatory as it propagates. The other one is the Ahkmediev breather (AB) [7] who is localized in the longitudinal dimension while oscillating along the transversal direction. Interestingly, as the oscillating period becomes infinity, both types of breathers can reduce to the Peregrine soliton [8], which is localized in both space and time. To date, because of their fundamental interests and practical implications, both breathers, including their reduced Peregrine soliton state, have become a hot topic, either theoretical [9–13] or experimental [14,15], at the cutting edge of nonlinear optics. Generally, the generation of optical breathers uses far-off-resonant mechanisms and high-intensity optical fields [2,15] which, as a result, cause a group velocity close to the light speed in vacuum.

In the past decades, there have been significant achievements concerning the propagation of electromagnetic waves in highly resonant media [16–22]. Among them, an important quantum interference effect known as electromagnetically induced transparency (EIT) was uncovered [23,24], by which the light pulses are allowed to propagate through an otherwise opaque atomic medium. Due to this EIT effect, the light-matter interaction process may exhibit some unique properties such as reducing the group velocity of light pulses [25,26], enhancing the Kerr nonlinearity [27,28], and lasing without population inversion [29]. In addition, ultraslow ordinary optical solitons were predicted to exist in the three-level [30,31] and four-level [32,33] atomic media. Also, the weak-light KM solitons and ABs were found to occur in such highly resonant media, within the framework of the nonlinear Schrödinger (NLS) equation [34–36].

#422914 https://doi.org/10.1364/OSAC.422914
Journal © 2021 Received 16 Feb 2021; revised 20 Apr 2021; accepted 22 Apr 2021; published 3 May 2021

OSA CONTINUUM

In this article, we will investigate the formation of KM solitons and ABs in a cold three-level atomic medium exposed to a probe field of nanosecond pulse duration. Within the integrable Hirota equation framework, we obtain for the first time the exact KM soliton and AB solutions. We then confirm by numerical simulations that both types of breathers are stable against non-integrable perturbations caused by the nonvanishing decay rates of atomic states and reveal that these breathers thus generated can propagate at a quite low group velocity.

2. Model, multiscale method, and generalized NLS equation

For our study, let us start with a lifetime broadened three-state atomic system that interacts with a weak pulsed probe field $E_p(\mathbf{r},t) = (\hbar/D_0)\Omega_p \exp[i\omega_p(z/c-t)] + c.c.$ (central frequency ω_p, Rabi frequency $2\Omega_p$) tuned to the transition $|1\rangle \rightarrow |3\rangle$ and a strong continuous-wave (cw) control field (angular frequency ω_c, Rabi frequency $2\Omega_c$) tuned to the transition $|2\rangle \rightarrow |3\rangle$ (see Fig. 1). Here $\hbar$ is the Planck constant divided by 2π, D_0 the dipole moment for the transition $|1\rangle \rightarrow |3\rangle$, and $c.c.$ is the shorthand of the complex conjugate terms. As a cold atomic medium is adopted here, we preclude the atomic collisions and Doppler broadening effect. Therefore, in the interaction picture and under the slowly varying envelope and rotating-wave approximations, the atomic equations for motion and the wave equation for the time-dependent probe field, often termed Maxwell–Bloch (MB) equations, can be expressed as [31]

$$(i\frac{\partial}{\partial t} + \Delta_2 + i\gamma_2)A_2 + \Omega_c^* A_3 = 0, \tag{1}$$

$$(i\frac{\partial}{\partial t} + \Delta_3 + i\gamma_3)A_3 + \Omega_p A_1 + \Omega_c A_2 = 0, \tag{2}$$

$$i(\frac{\partial}{\partial z} + \frac{1}{c}\frac{\partial}{\partial t})\Omega_p + \frac{c}{2\omega_p}(\frac{\partial^2}{\partial x^2} + \frac{\partial^2}{\partial y^2})\Omega_p + \kappa A_3 A_1^* = 0, \tag{3}$$

where A_j $(j = 1, 2, 3)$ are the probability amplitudes of atomic states $|j\rangle$ and the asterisk stands for complex conjugate. These probability amplitudes may evolve with the propagation distance z, the time t, and the transverse coordinates x and y, but need to obey the conservation condition:

$$\sum_{j=1}^{3} |A_j|^2 = 1, \tag{4}$$

which means the total probability of finding an atom in any of three states is equal to unity. While the parameters γ_j $(j = 2, 3)$ denote the decay rates of the state $|j\rangle$ of energy eigenvalue ϵ_j, $\Delta_3 = \omega_p - \epsilon_3/\hbar$ and $\Delta_2 = \omega_p - \omega_c - \epsilon_2/\hbar$ represent the one-photon detuning between the states $|1\rangle$ and $|3\rangle$ and the two-photon detuning between the states $|1\rangle$ and $|2\rangle$, respectively, where the energy of the ground state has been set zero, i.e., $\epsilon_1 = 0$. Of course the one-photon detuning Δ_c for the control field tuned to the transition $|2\rangle \rightarrow |3\rangle$ reads as $\Delta_c = \omega_c - (\epsilon_3 - \epsilon_2)/\hbar = \Delta_3 - \Delta_2$. In addition, $\kappa = 2\pi N\omega_p|D_0|^2/(\hbar c)$ signifies the strength of coherent coupling, with N being the concentration of three-level atoms and c the speed of light in vacuum.

We now use a standard multiscale approach [37] to derive the nonlinear envelope equation describing the evolution of the weak probe optical field, under the assumption of a small population depletion of the ground state. To this end, one can perform the asymptotic expansions $A_j = \sum_{m=0}^{\infty} \varepsilon^m a_j^{(m)}$ and $\Omega_p = \sum_{n=1}^{\infty} \varepsilon^n \Omega_p^{(n)}$, and let all quantities therein be the functions of $z_\iota = \varepsilon^\iota z$ $(\iota = 0, \ldots, 3)$, $t_1 = \varepsilon t$, $x_1 = \varepsilon x$, and $y_1 = \varepsilon y$. It should be noted that there is a slight difference between our multiscale variables and those used in [31,34]. Then, inserting these expanded formulas into Eqs. (1)–(4), followed by equating the coefficients of ε^m to zero, one

OSA CONTINUUM

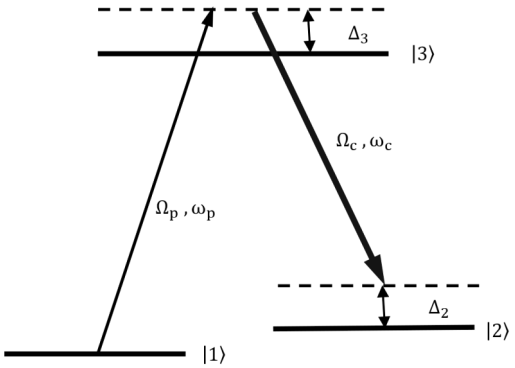

Fig. 1. The excitation scheme of a Λ-type lifetime broadened three-state atomic system interacting with a pulsed probe field (central frequency ω_p, Rabi frequency $2\Omega_p$) and a strong cw control field (angular frequency ω_c, Rabi frequency $2\Omega_c$).

can obtain a succession of linear but nonhomogeneous equations involving $a_j^{(m)}$ and $\Omega_p^{(n)}$. The preceding low-order equations can be written as

$$(i\gamma_2 + \Delta_2)a_2^{(\ell)} + \Omega_c^* a_3^{(\ell)} = -i\frac{\partial a_2^{(\ell-1)}}{\partial t_1}, \tag{5}$$

$$(i\gamma_3 + \Delta_3)a_3^{(\ell)} + \Omega_p^{(\ell)} + \Omega_c a_2^{(\ell)} = M^{(\ell-1)} - i\frac{\partial a_3^{(\ell-1)}}{\partial t_1}, \tag{6}$$

$$i\frac{\partial}{\partial z_0}\Omega_p^{(\ell)} + \kappa a_3^{(\ell)} = N^{(\ell-1)} - i(\frac{\partial}{\partial z_1} + \frac{1}{c}\frac{\partial}{\partial t_1})\Omega_p^{(\ell-1)}, \tag{7}$$

where $\ell = 1, \ldots, 4$, $a_1^{(0)} = 1$, $a_2^{(0)} = a_3^{(0)} = 0$, $\Omega_p^{(0)} = 0$, $M^{(0)} = M^{(1)} = 0$, $M^{(2)} = -\Omega_p^{(1)} a_1^{(2)}$, $M^{(3)} = -\Omega_p^{(1)} a_1^{(3)} - \Omega_p^{(2)} a_1^{(2)}$, $N^{(0)} = N^{(1)} = 0$, $N^{(2)} = -\kappa a_3^{(1)} a_1^{(2)*} - i\frac{\partial}{\partial z_2}\Omega_p^{(1)} - \frac{c}{2\omega_p}(\frac{\partial^2}{\partial x_1^2} + \frac{\partial^2}{\partial y_1^2})\Omega_p^{(1)}$, and $N^{(3)} = -\kappa a_3^{(2)} a_1^{(2)*} - \kappa a_3^{(1)} a_1^{(3)*} - i\frac{\partial}{\partial z_3}\Omega_p^{(1)} - i\frac{\partial}{\partial z_2}\Omega_p^{(2)} - \frac{c}{2\omega_p}(\frac{\partial^2}{\partial x_1^2} + \frac{\partial^2}{\partial y_1^2})\Omega_p^{(2)}$.

Obviously, the system of linear Eqs. (5)–(7) can be solved in an iterative yet exact manner, with the help of the conservation relation (4). After some algebra, we find $\Omega_p^{(1)} = F(z_1, z_2, z_3, t_1, x_1, y_1)\exp(iK_0 z_0)$ and $\Omega_p^{(n)} = 0$ for $n \geqslant 2$, where F is the complex amplitude and $K_0 = \kappa d_2/D$ is the complex wave number, with $D = |\Omega_c|^2 - d_2 d_3$ and $d_j = i\gamma_j + \Delta_j$ $(j = 2, 3)$. In terms of the function F and its derivatives, the probability amplitudes $a_j^{(m)}$ can also be exactly defined (we do not present their explicit expressions here, for the sake of brevity). Recalling that $\Omega_p = \varepsilon\Omega_p^{(1)} = U\exp[i\mathrm{Re}(K_0)z_0]$, where $U = \epsilon F\exp(-\alpha z_0)$, with $\alpha = \mathrm{Im}(K_0)$ and Im standing for the imaginary part, is the envelope amplitude, we find, after returning to the original variables (z, t, x, y), that the nonlinear envelope equation for U can read as

$$\begin{aligned} &i(U_z + K_1 U_t + \alpha U) - \frac{K_2}{2}U_{tt} + \frac{c}{2\omega_p}(U_{xx} + U_{yy}) - \gamma|U|^2 U \\ &\quad = i\left[\frac{K_3}{6}U_{ttt} + \beta_1 U(|U|^2)_t + (\beta_2 - \beta_1)|U|^2 U_t\right], \end{aligned} \tag{8}$$

where the subscripts for U denote partial derivatives, and the equation coefficients are given by

$$K_1 = \frac{1}{c} + \frac{\kappa(|\Omega_c|^2 + d_2^2)}{D^2}, \tag{9}$$

OSA CONTINUUM

$$K_2 = \frac{2\kappa d_2}{D^2} + \frac{2(d_2+d_3)}{D}(K_1 - \frac{1}{c}), \tag{10}$$

$$K_3 = \frac{6}{D}(K_1 - \frac{1}{c}) + \frac{3K_2}{D}(d_2+d_3), \tag{11}$$

$$\gamma = \frac{\kappa d_2(|\Omega_c|^2 + |d_2|^2)}{D|D|^2}, \tag{12}$$

$$\beta_1 = \frac{|\Omega_c|^2 + |d_2|^2}{2|D|^2}(K_1 - \frac{1}{c}) - \frac{\kappa|d_2|^2}{D|D|^2} - \frac{d_2(d_2+d_3^*)}{D^2}(K_1^* - \frac{1}{c}), \tag{13}$$

$$\beta_2 = \frac{5(|\Omega_c|^2 + |d_2|^2) - 2D}{2|D|^2}(K_1 - \frac{1}{c}) + \frac{\kappa d_2^2}{D|D|^2}. \tag{14}$$

We should point out that our Eq. (8) obtained here is a direct result of Eqs. (5)–(7) without any further approximations; it seems to be similar in form to Eq. (18) derived in [31], but involves different equation coefficients defined by Eqs. (9)–(14). It is apparent that these equation coefficients are all complex (because of the introduction of the complex d_2 and d_3) and can be separated into the real and imaginary parts, namely, $K_j = K_j' + iK_j''$ ($j = 1, 2, 3$), $\gamma = \gamma' + i\gamma''$, and $\beta_{1,2} = \beta_{1,2}' + i\beta_{1,2}''$. Usually, $V_g = 1/K_1'$ gives the group velocity of the probe field. In this regard, Eq. (8) becomes an analog of the (3+1)D complex Ginzburg-Landau equation [38], comprising the spectral filtering denoted by K_2'', the third-order spectral correction by K_3'', the linear loss by α, and the nonlinearity gain by γ''. However, in a very short distance and considering that $\Delta_2 \gg \gamma_2$ and $\Delta_3 \gg \gamma_3$, which is accessible by typical alkali atoms, these extra effects resulting from the imaginary parts of the coefficients will become insignificant and thus can be neglected. Under the circumstances, Eq. (8) can be reduced to the generalized NLS equation, whose coefficients are still given by Eqs. (9)–(14), but with d_j being replaced by Δ_j. For this case, one can obtain the group velocity V_g of the weak probe field:

$$V_g = \frac{c}{1 + c\kappa(|\Omega_c|^2 + \Delta_2^2)/(|\Omega_c|^2 - \Delta_2\Delta_3)^2}, \tag{15}$$

which depends on the coupling strength (κ), the input power of the coupling beam ($\propto |\Omega_c|^2$), and the one- and two-photon detunings ($\Delta_{2,3}$). It suggests that, for obtaining a significantly low group velocity, sufficiently small one- and two-photon detunings yet still predominating over the decay rates, along with a moderately weak control field, are favorable. This is a trade-off process, whose outcome is unavailable with the conventional perfectly resonant EIT scheme under weak driving conditions, in which exceptionally low light speeds can be observed [25,26].

3. Dynamics of KM solitons and ABs and numerical simulations

More interestingly, if we neglect the spatial diffraction effect and the linear loss, which holds true for a propagation distance of a few dispersion lengths $L_D = \tau_0^2/|K_2|$, and let further

$$\beta_1 \simeq 0, \quad \beta_2 - \beta_1 = \frac{\gamma K_3}{K_2}, \tag{16}$$

Equation (8) becomes the celebrated Hirota equation:

$$iU_z - \frac{K_2}{2}U_{\tau\tau} - \gamma|U|^2U - iK_3\left(\frac{1}{6}U_{\tau\tau\tau} + \frac{\gamma}{K_2}|U|^2U_\tau\right) = 0, \tag{17}$$

where $\tau = t - z/V_g$ is the retarded time in a frame comoving with V_g. When substituting the specified parameters into the relations (16), one can figure out the experimental parameter

OSA CONTINUUM

conditions that may lead to the above Hirota equation:

$$\Delta_2 \simeq 3\Delta_3, \qquad |\Omega_c| = \sqrt{\frac{(\Delta_2 + 3\Delta_3)\Delta_2^2}{\Delta_2 - \Delta_3}}. \tag{18}$$

The first of Eqs. (18) actually requires that the one-photon detuning Δ_c for the control field tuned to the transition $|2\rangle \rightarrow |3\rangle$ should be negative twice that for the probe field tuned to the transition $|1\rangle \rightarrow |3\rangle$, i.e. $\Delta_c = -2\Delta_3$. The second of Eqs. (18) imposes a restriction on the Rabi frequency Ω_c and thus on the input power of the control field, which can also be accessible for current commercial cw lasers. An inspection of these two parameter conditions reveals that if Δ_3>0, the atomic medium entails the normal dispersion and self-defocusing nonlinearity, otherwise it entails the anomalous dispersion and self-focusing nonlinearity, i.e., in whatever case, γ/K_2>0.

The Hirota Eq. (17) is integrable and can be solved by many analytical methods [39,40]. It admits plenty of exact solutions, such as solitons, rogue waves, and breathers [41,42]. Of special interest are the KM and AB solutions, either of which arises from the modulation instability of the unstable background field [2]. By means of the bilinear Hirota approach [39] and starting from the seeding plane-wave solution

$$U_0 = \sqrt{P}\exp(ikz + i\omega\tau), \tag{19}$$

with $k = -\frac{1}{6}K_3\omega^3 + \frac{1}{2}K_2\omega^2 + \eta$ and $\eta = \gamma P(K_3\omega/K_2 - 1)$, we obtain for the first time, to the best of our knowledge, the KM soliton solution, in an elegant compact form

$$U_{\mathrm{KM}} = \frac{\cos(gz - 2i\phi) - \cosh(\phi)\cosh\left[q(z\chi + \tau)\right]}{\cos(gz) - \cosh(\phi)\cosh\left[q(z\chi + \tau)\right]}U_0, \tag{20}$$

where ϕ is a real free parameter defining the oscillating frequency, P is the background intensity, ω is the detuning from the central frequency ω_p, $g = \eta\sinh(2\phi)$, $q = 2\sqrt{\gamma P/K_2}\sinh(\phi)$, and $\chi = (\gamma PK_3/K_2)[1 + \frac{2}{3}\sinh(\phi)^2] - K_3\omega^2/2 + K_2\omega$. In a similar fashion, the AB solution can be found to be

$$U_{\mathrm{AB}} = \frac{\cosh(gz - 2i\phi) - \cos(\phi)\cos\left[q(z\chi + \tau)\right]}{\cosh(gz) - \cos(\phi)\cos\left[q(z\chi + \tau)\right]}U_0, \tag{21}$$

where we use now $g = \eta\sin(2\phi)$, $q = 2\sqrt{\gamma P/K_2}\sin(\phi)$, and $\chi = (\gamma PK_3/K_2)[1 - \frac{2}{3}\sin(\phi)^2] - K_3\omega^2/2 + K_2\omega$. One can readily show that, as the frequency parameter ϕ approaches zero, both the KM solution (20) and the AB solution (21) will boil down to the same rational solution [42]

$$U_{\mathrm{PS}} = \left[1 - \frac{2i\eta z + 1}{\eta^2 z^2 + \gamma P(z\chi + \tau)^2/K_2 + 1/4}\right]U_0, \tag{22}$$

where $\chi = \gamma PK_3/K_2 - K_3\omega^2/2 + K_2\omega$. This solution, when γ/K_2>0 is met, represents nothing less than a Peregrine soliton [8], featuring a three-fold-amplitude peak on a finite background and two deep troughs on each side.

It follows easily that the KM soliton solution (20) oscillates along the propagation direction $z\chi + \tau = 0$, with the amplitude of all peaks as high as $[1 + 2\cosh(\phi)]\sqrt{P}$ ($\geqslant 3\sqrt{P}$), but located on $(\tau_j, z_j) = (-2j\pi\chi/g, 2j\pi/g)$, $(j = 0, \pm1, \pm2, \ldots)$. By contrast, the AB solution (21) is found to oscillate along the transversal (i.e., $z = 0$) direction, with its peaks being located on $(\tau_j, z_j) = (2j\pi/q, 0)$, $(j = 0, \pm1, \pm2, \ldots)$ and as high as $[1 + 2\cos(\phi)]\sqrt{P}$ ($\leqslant 3\sqrt{P}$). On the other hand, the peak power associated to the incident pulsed probe beam of cross-section area S_0 can be calculated by $P_{\mathrm{peak}} = 2\epsilon_0 cn_p S_0(\hbar/D_0)^2 P$, where ϵ_0 is the permittivity of free space and $n_p = 1 + cK_0/\omega_p$ is the phase refractive index experienced by the probe field. Albeit P is a free parameter in Eqs. (20) and (21), there is a practical requirement on the input peak power

OSA CONTINUUM

P_{peak} for forming stable KM solitons and ABs within a limited-size cell of alkali atom gases. Besides, we need to point out that although both the KM and AB solutions discussed above bear a similarity to the corresponding ones of the standard NLS equation [35,36,42], they can describe more accurately the propagation of the probe pulses of duration down to the picosecond order, due to the inclusion of the parameters η and χ, which are related to the third-order dispersion (K_3) and self-steepening ($\gamma K_3/K_2$) effects.

We now consider some numerical examples to demonstrate these two types of breathers in a typical alkali (Rubidium 87 D_2 transition, say) atomic system, where the coupling strength is $\kappa = 1.0 \times 10^9 \text{cm}^{-1}\text{s}^{-1}$ and the decay rates are $\Gamma_2 = 2\gamma_2 = 10$kHz and $\Gamma_3 = 2\gamma_3 = 5$MHz [31]. When a weak probe pulse of 0.12 cm beam diameter (central wavelength $\lambda_p = 2\pi c/\omega_p = 780$ nm, pulse duration $\tau_0 = 30$ ns, peak power $P_{\text{peak}} = 700$ mW or $P = 6.25 \times 10^{15}$ s^{-2}) was launched into the medium (let $D_0 = 2.1 \times 10^{-27}$ cm C), we tuned the detunings by $\Delta_3 = 50$MHz and $\Delta_2 = 3\Delta_3 = 150$MHz, which are much larger than the decay rates, and adjusted the Rabi frequency of the control field by $2\Omega_c = 6\sqrt{3}\Delta_3 = 519.6$MHz, which will be significantly greater than that of the probe field, $2\sqrt{P} = 158$ MHz. In fact, for a typical nanosecond pulse laser of 100 kHz repetition rate, the above peak power value corresponds to 2.1mW average output power, which is also much less than the nominal average power of most current commercial 780nm cw lasers, thereby justifying the choice of the above adopted parameters. With these characteristic values, one can calculate the equation coefficients as $K_1 = 2.5 \times 10^{-6}$ sm^{-1}, $K_2 = 2.5 \times 10^{-14}$ s^{2}m^{-1}, $K_3 = 5.0 \times 10^{-22}$ s^{3}m^{-1}, $\gamma = 6.25 \times 10^{-15}$ s^{2}m^{-1}, $\beta_1 = 0$, and $\beta_2 = 1.25 \times 10^{-22}$ s^{3}m^{-1}, where the insignificant imaginary parts are dropped. Then the dispersion length is found to be $L_D = 3.6$ cm, which has been made to equal to the nonlinearity length $L_{\text{NL}} = 1/(\gamma P)$ in order to favor the formation of fundamental soliton. The analytical dynamics of the KM soliton solution (20) and the AB solution (21) are shown in Figs. 2(a) and 2(b), respectively, with ϕ and ω being specified in the caption. It is shown that the KM soliton oscillates periodically along the z axis, whereas the AB oscillates periodically along the τ axis, as stated above, both propagating with a group velocity of $V_g = c/751$. When $\phi = 0$, the recurring peaks of both breathers disappear, left with only one single peak and two side troughs, namely, a Peregrine soliton structure that has been shown in Fig. 2(c). As indicated by the red cross-section profiles of the framed patterns at $z = 0$, the peak amplitude of the KM is always larger than that of the Peregrine soliton, but the latter is always larger than that of the AB, no matter what parameters are used.

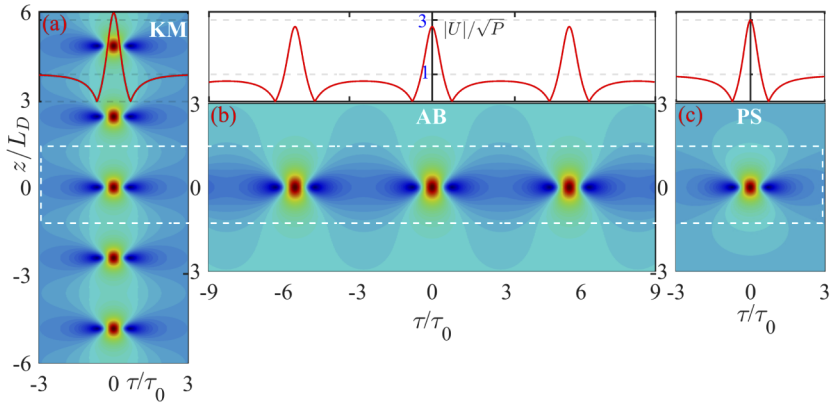

Fig. 2. Contour plots of the normalized field amplitude of (a) a KM soliton, (b) an AB, and (c) a Peregrine soliton versus dimensionless distance z/L_D and time τ/τ_0, obtained with different ϕ and ω values: (a) $\phi = 1/2$, $\omega = 1.29 \times 10^8$ s^{-1}, (b) $\phi = 1/2$, $\omega = 1.22 \times 10^8$ s^{-1}, and (c) $\phi = 0$, $\omega = 1.25 \times 10^8$ s^{-1}.The red curves show the cross-section profiles $|U(z = 0, \tau)|/\sqrt{P}$ of the patterns framed by the white box.

OSA CONTINUUM

Lastly, one may wonder whether both the KM soliton and the AB shown in Fig. 2 are stable against perturbations, even when the imaginary parts of equation coefficients are taken into account. To clarify this concern, we numerically integrate Eq. (17) to unwrap the KM soliton and AB dynamics from an initial profile defined by the analytical solution (20) at $z = -3L_D$ and by the solution (21) at $z = -2L_D$, respectively, using a split-step Fourier method [9,10]. Here we particularly remark that one may simulate the original MB Eqs. (1)–(3) for more accurate results, but basically, for a very short propagation distance, an efficient simulation of Eq. (17) will suffice for our present purpose. Typical simulation results are shown in Fig. 3, where we have considered the non-integrable perturbations, that is, violating the integrability of Eq. (17) by use of a set of complex coefficients that is caused by the nonvanishing decay rates of atomic states. It is exhibited that our KM soliton and AB solutions are still robust against such non-integrable perturbations, within a distance of a few dispersion lengths. More interestingly, in Fig. 3(a), there also appears a partial AB dynamics at around $z = 2L_D$, which agrees well with its analytical solution shown in the middle of picture (see the patterns framed by the white box). This excited AB tends to interfere with the original KM soliton and eventually distorts it.

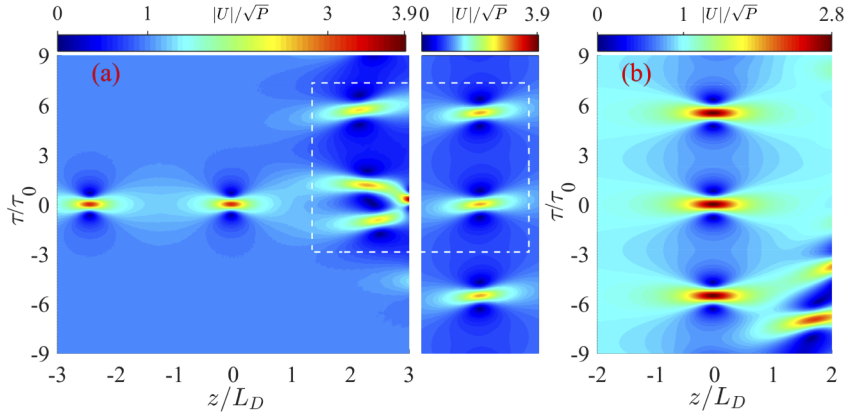

Fig. 3. Numerical excitations of (a) the KM soliton and (b) the AB that have been shown in Fig. 2(a) and 2(b), respectively, by integrating Eq. (17) with complex coefficients. The middle contour plot between (a) and (b) gives the analytical solution of AB, using the same ϕ and ω as in (a).

4. Conclusion

In conclusion, we investigated the formation of the KM solitons and ABs in a cold three-level atomic medium, within the framework of the Hirota equation that has comprised the third-order dispersion and self-steepening effects seen by nanosecond probe pulses. We revealed the unique amplitude and oscillatory characteristics associated with these breathers and confirmed numerically their stability against non-integrable perturbations. It was shown that such types of breathers can propagate at a quite low group velocity. However, for probe pulses of shorter (picosecond, say) duration, our results developed here still apply. In the latter situation, the bandwidth of incident pulses will fall outside the EIT transparency window seriously, leading to a light-matter interaction in the proximity of the off-resonant regime and consequently making the group velocity of probe pulses closer to the light speed c. We envision that these results may shed some light on how extreme rogue waves form in highly resonant media.

Funding. National Natural Science Foundation of China (11474051, 11974075); Scientific Research Foundation of the Graduate School of Southeast University (YBPY1872).

Disclosures. The authors declare no conflicts of interest.

OSA CONTINUUM

References

1. A. Chabchoub, B. Kibler, J. M. Dudley, and N. Akhmediev, "Hydrodynamics of periodic breathers," Phil. Trans. R. Soc. A **372**(2027), 20140005 (2014).
2. B. Kibler, A. Chabchoub, A. Gelash, N. Akhmediev, and V. E. Zakharov, "Superregular breathers in optics and hydrodynamics: omnipresent modulation instability beyond simple periodicity," Phys. Rev. X **5**(4), 041026 (2015).
3. D. R. Solli, C. Ropers, P. Koonath, and B. Jalali, "Optical rogue waves," Nature (London) **450**(7172), 1054–1057 (2007).
4. J. M. Dudley, F. Dias, M. Erkintalo, and G. Genty, "Instabilities, breathers and rogue waves in optics," Nat. Photonics **8**(10), 755–764 (2014).
5. E. A. Kuznetsov, "Solitons in a parametrically unstable plasma," Sov. Phys.–Dokl. **22**(9), 507–508 (1977).
6. Y.-C. Ma, "The perturbed plane-wave solutions of the cubic Schrödinger equation," Stud. Appl. Math. **60**(1), 43–58 (1979).
7. N. N. Akhmediev and V. I. Korneev, "Modulation instability and periodic solutions of the nonlinear Schrödinger equation," Theor. Math. Phys. **69**(2), 1089–1093 (1986).
8. D. H. Peregrine, "Water waves, nonlinear Schrödinger equations and their solutions," J. Aust. Math. Soc. Ser. B: Appl. Math. **25**(1), 16–43 (1983).
9. S. Chen, Y. Ye, J. M. Soto-Crespo, P. Grelu, and F. Baronio, "Peregrine Solitons Beyond the Threefold Limit and Their Two-Soliton Interactions," Phys. Rev. Lett. **121**(10), 104101 (2018).
10. S. Chen, C. Pan, P. Grelu, F. Baronio, and N. Akhmediev, "Fundamental Peregrine Solitons of Ultrastrong Amplitude Enhancement through Self-Steepening in Vector Nonlinear Systems," Phys. Rev. Lett. **124**(11), 113901 (2020).
11. L.-C. Zhao, L. Ling, and Z.-Y. Yang, "Mechanism of Kuznetsov-Ma breathers," Phys. Rev. E **97**(2), 022218 (2018).
12. F. Baronio, "Akhmediev breathers and Peregrine solitary waves in a quadratic medium," Opt. Lett. **42**(9), 1756–1759 (2017).
13. F. Baronio, S. Chen, and S. Trillo, "Resonant radiation from Peregrine solitons," Opt. Lett. **45**(2), 427–430 (2020).
14. B. Kibler, J. Fatome, C. Finot, G. Millot, F. Dias, G. Genty, N. Akhmediev, and J. M. Dudley, "The Peregrine soliton in nonlinear fibre optics," Nat. Phys. **6**(10), 790–795 (2010).
15. B. Kibler, J. Fatome, C. Finot, G. Millot, G. Genty, B. Wetzel, N. Akhmediev, F. Dias, and J. M. Dudley, "Observation of Kuznetsov-Ma soliton dynamics in optical fibre," Sci. Rep. **2**(1), 463 (2012).
16. L. Allen and J. H. Eberly, *Optical Resonance and Two-Level Atoms* (Wiley, 1975).
17. M. Fleischhauer, A. Imamoglu, and J. P. Marangos, "Electromagnetically induced transparency: Optics in coherent media," Rev. Mod. Phys. **77**(2), 633–673 (2005).
18. S. Chen, Y. Ye, F. Baronio, Y. Liu, X.-M. Cai, and P. Grelu, "Optical Peregrine rogue waves of self-induced transparency in a resonant erbium-doped fiber," Opt. Express **25**(24), 29687–29698 (2017).
19. J. Liu, C. Hang, and G. Huang, "Weak-light vector rogue waves, breathers, and their Stern-Gerlach deflection via electromagnetically induced transparency," Opt. Express **25**(19), 23408–23423 (2017).
20. J. Guan, C. J. Zhu, C. Hang, and Y. P. Yang, "Generation and propagation of hyperbolic secant solitons, Peregrine solitons, and breathers in a coherently prepared atomic system," Opt. Express **28**(21), 31287–31296 (2020).
21. C. Shou and G. Huang, "Storage, Splitting, and Routing of Optical Peregrine Solitons in a Coherent Atomic System," Front. Phys. **9**, 594680 (2021).
22. Z. Chen and J. Zeng, "Localized gap modes of coherently trapped atoms in an optical lattice," Opt. Express **29**(3), 3011 (2021).
23. S. E. Harris, J. E. Field, and A. Imamoglu, "Nonlinear Optical Processes Using Electromagnetically induced transparency," Phys. Rev. Lett. **64**(10), 1107–1110 (1990).
24. S. E. Harris, "Electromagnetically induced transparency," Phys. Today **50**(7), 36–42 (1997).
25. L. V. Hau, S. E. Harris, Z. Dutton, and C. H. Behroozi, "Light speed reduction to 17 metres per second in an ultracold atomic gas," Nature (London, U. K.) **397**(6720), 594–598 (1999).
26. C. Liu, Z. Dutton, C. H. Behroozi, and L. V. Hau, "Observation of coherent optical information storage in an atomic medium using halted light pulses," Nature (London, U. K.) **409**(6819), 490–493 (2001).
27. H. Schmidt and A. Imamoglu, "Giant Kerr nonlinearities obtained by electromagnetically induced transparency," Opt. Lett. **21**(23), 1936–1938 (1996).
28. H. Wang, D. Goorskey, and M. Xiao, "Enhanced Kerr Nonlinearity via Atomic Coherence in a Three-Level Atomic System," Phys. Rev. Lett. **87**(7), 073601 (2001).
29. G. G. Padmabandu, G. R. Welch, I. N. Shubin, E. S. Fry, D. E. Nikonov, M. D. Lukin, and M. O. Scully, "Laser Oscillation without Population Inversion in a Sodium Atomic Beam," Phys. Rev. Lett. **76**(12), 2053–2056 (1996).
30. Y. Wu and L. Deng, "Ultraslow bright and dark optical solitons in a cold three-state medium," Opt. Lett. **29**(17), 2064–2066 (2004).
31. G. Huang, L. Deng, and M. G. Payne, "Dynamics of ultraslow optical solitons in a cold three-state atomic system," Phys. Rev. E **72**(1), 016617 (2005).
32. Y. Wu and L. Deng, "Ultraslow optical solitons in a cold four-state medium," Phys. Rev. Lett. **93**(14), 143904 (2004).
33. L.-G. Si, W.-X. Yang, and X. Yang, "Ultraslow temporal vector optical solitons in a cold four-level tripod atomic system," J. Opt. Soc. Am. B **26**(3), 478–486 (2009).
34. J. Liu, C. Hang, and G. Huang, "Weak-light rogue waves, breathers, and their active control in a cold atomic gas via electromagnetically induced transparency," Phys. Rev. A **93**(6), 063836 (2016).

OSA CONTINUUM

35. S. Asgarnezhad-Zorgabad, R. Sadighi-Bonabi, and B. C. Sanders, "Excitation and propagation of surface polaritonic rogue waves and breathers," Phys. Rev. A **98**(1), 013825 (2018).
36. K. M. Devi, G. Kumar, and A. K. Sarma, "Surface polaritonic solitons and breathers in a planar plasmonic waveguide structure via electromagnetically induced transparency," J. Opt. Soc. Am. B **36**(8), 2160–2166 (2019).
37. A. Jeffrey and T. Kawahara, *Asymptotic Methods in Nonlinear Wave Theory* (Pitman, 1982).
38. Z. Li, L. Li, H. Tian, G. Zhou, and K. H. Spatschek, "Chirped Femtosecond Solitonlike Laser Pulse Form with Self-Frequency Shift," Phys. Rev. Lett. **89**(26), 263901 (2002).
39. R. Hirota, "Exact envelope-soliton solutions of a nonlinear wave equation," J. Math. Phys. **14**(7), 805–809 (1973).
40. A. Ankiewicz, J. M. Soto-Crespo, and N. Akhmediev, "Rogue waves and rational solutions of the Hirota equation," Phys. Rev. E **81**(4), 046602 (2010).
41. Y. Tao and J. He, "Multisolitons, breathers, and rogue waves for the Hirota equation generated by the Darboux transformation," Phys. Rev. E **85**(2), 026601 (2012).
42. S. Chen, F. Baronio, J. M. Soto-Crespo, P. Grelu, and D. Mihalache, "Versatile rogue waves in scalar, vector, and multidimensional nonlinear systems," J. Phys. A: Math. Theor. **50**(46), 463001 (2017).